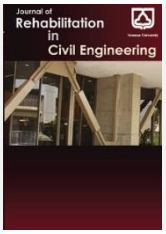

Journal of Rehabilitation in Civil Engineering

Journal homepage: https://civiljournal.semnan.ac.ir/

Influence of Aggregate Gradation and Pore Structure on Porous Asphalt Mixture Permeability and Resilient Modulus

Gummadi Chiranjeevi [1*]; S Shankar [2]

1. Research Scholar, Department of Civil Engineering, Transportation Division, National Institute of Technology, Warangal - 506004, India
2. Associate Professor, Department of Civil Engineering, Transportation Division, National Institute of Technology, Warangal -506004, India
* Corresponding author: *gc720028@student.nitw.ac.in*

ARTICLE INFO

Article history:
Received: 22 March 2024
Revised: 02 August 2024
Accepted: 16 January 2025

Keywords:
Porous asphalt pavement;
Permeability;
Resilient-modulus;
Drainage capacity;
Air void structure;
Stormwater.

ABSTRACT

A porous asphalt mixture (PAM) is distinguished by its different porous structures, which allow water to move through it as quickly as possible, making drainage an essential component. Porous asphalt pavement (PAP) can maintain its permeability because the mixture contains voids that are interconnected with one another. Permeability, on the other hand, decreases as the proportion of particles in the gradation and the level of compaction increases. To generate various air-void structures, permeability was evaluated with specimens made from varying sizes and shapes of aggregates. The equipment that was used for this research was specifically designed. When compared directly with permeability, the findings indicate that the combination of multiple forms is not directly comparable. The permeability of PAM was observed to be affected by a variety of air void densities, which were observed. While there was a beneficial influence on permeability, there was a negative impact on the Resilient Modulus (MR), which was detected when there was an increase in the void content. The amount of air voids in the mixture substantially impacts the performance of porous asphalt mixtures. Open-Gr-I viscosity grade (VG30) bitumen has a permeability value of 0.394 cm/s, and the resilience modulus value for open-Gr-II mixtures that use a modified binder is 3494 MPa. Both of these values are relative to the permeability value. The drainage and stiffness metrics for the several combinations investigated in this study were considerably impacted by the gradation, the kind of binder, and the temperature conditions. Stormwater management is possible in PAP and improves the groundwater table.

E-ISSN: 2345-4423

How to cite this article:
Chiranjeevi, G. and Shankar, S. (2026). Influence of Aggregate Gradation and Pore Structure on Porous Asphalt Mixture Permeability and Resilient Modulus. Journal of Rehabilitation in Civil Engineering, 14(1), 2027 https://doi.org/10.22075/jrce.2024.33599.2027

1. Introduction

Porous asphalt mixtures are increasingly popular due to their benefits in driver comfort and safety. These pavements allow water to drain off the road surface, significantly reducing hydroplaning and decreasing the risk of accidents, particularly on high-speed roads, Figure 1 shows the Basis for the adoption of porous asphalt pavement. [1,2]. The porous structure also helps reduce noise as the pores within the asphalt mixture absorb sound waves. The internal connectivity of these pores largely determines the performance of permeable pavement. Open-graded mixtures, which incorporate a significant amount of large aggregates, are typically used to maintain the permeability of the pavement layer. [3–6].

There are two common approaches for designing porous asphalt mixtures to ensure the presence of connected voids: regulating the total air void content, also known as interconnected air voids, and measuring the mixture's permeability to reflect the connectivity of the internal voids. The total air void content gives an overall measure of the mixture's porosity. In contrast, permeability provides insights into the drainage capability of the mix, as well as the extent and size of void connectivity. It is crucial to assess the permeability of the porous asphalt mixture during the design phase to ensure its drainage, anti-skid, and noise reduction capabilities.[7–12].

Permeability and stiffness are key performance indicators for porous asphalt pavements. The permeability test is directly related to the air void content in the mixture, while the stiffness parameter indicates the mixture's horizontal deformation and ability to recover strain. The pavement layer is resilient modulus and depends on the compacted layer's indirect tensile strength (ITS) value, which is typically considered to be between 10-20% when conducting a Resilient Modules test. This test helps in assessing horizontal deformation and recoverable strains. [13–15].

The quieter nature of roads with porous asphalt surfaces is attributed to the dispersion of sound waves across the mixture's pores. The performance of porous asphalt road pavement is primarily influenced by the internal connectivity of the mixture's pores. The pore structure and connectivity significantly impact the internal permeability of compacted specimens. [16–21].

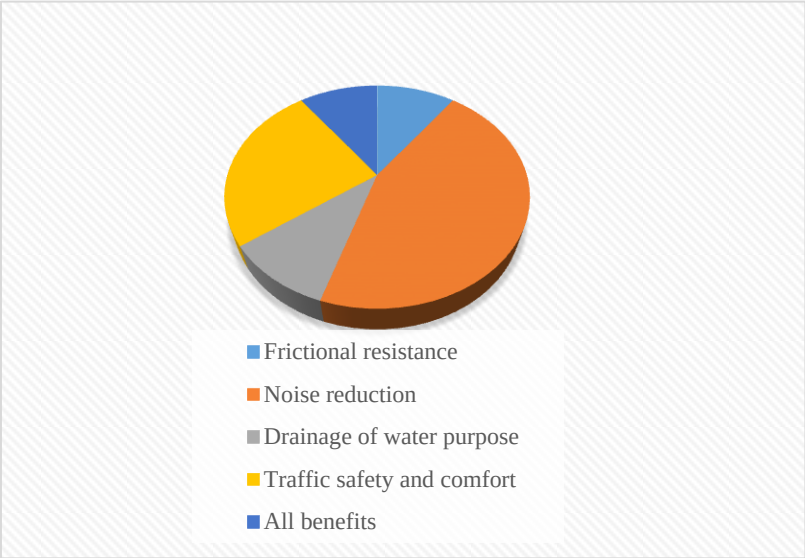

Fig. 1. Basis for the adoption of Porous asphalt pavement.

Porous asphalt paving technologies have been recognized globally as a reliable solution for sustainable drainage systems. These systems can incorporate permeable pavement, which includes porous asphalt. The porosity and pores in porous asphalt help eliminate many contaminants from stormwater runoff and reduce the risk of hydroplaning. The high levels of air void content contribute to its permeability,

resulting in lower stormwater flow on the pavement surface. This reduction in flow leads to fewer splashes and floods during rainy conditions, thereby enhancing road safety, improving visibility, reducing accident likelihood, and decreasing the danger of hydroplaning. The unique aspect of porous asphalt is its combination of stormwater treatment and control with vehicle functionality[22–25]. Rainfall duration significantly influences the sample's permeability [26].

Additionally, the open-graded structures of porous asphalt mixtures (PAM) offer excellent sound absorption, which helps reduce tire noise on the road surface. However, an open-graded mixture's resilient modulus and tensile strength are typically much lower than conventional dense-graded asphalt. This open structure also significantly reduces the mixture's durability. Aggregate gradation plays a crucial role in the performance of PAM. The resilient modulus test, often used to assess an asphalt material's stiffness, has shown that the crushed aggregate component influences the resilient modulus in the asphalt mixture. This has been demonstrated in large-scale, conventional tests.[27–30].

The resilient modulus of the asphalt specimens was evaluated using the Repeated Load Indirect Tensile Test (RLITT). This test is performed at low stress levels, with a maximum stress of ten percent of the breakthrough stress, to ensure the linear behavior of the materials. The test involves five pulses of haversine loading, with each pulse lasting for three thousand milliseconds. The total recoverable diametrical strain is measured along an axis perpendicular to the applied load. A Universal Testing Machine (UTM) is used for the RLITT, which includes a temperature-controlled chamber to maintain a consistent temperature throughout the test. Specimens are conditioned in this temperature for at least three to four hours before testing. The test specimens are cylindrical, measuring 65 mm in thickness and 100 mm in diameter, as recommended by various studies. [31,32].

Considering the economic and ecological aspects of improving asphalt binder performance is essential. Modified binders generally offer better performance.[33–35]. Moreover, in urban areas, the ability to filter contaminants from stormwater helps protect the environment and reduce runoff. [36,37]. However, evaluating the stiffness performance is a significant step in studying porous mixtures, enhancing the application of these materials in high-traffic conditions. This research's innovative aspect lies in combining highly modified asphalt with a porous asphalt mixture, resulting in excellent stiffness resistance and effective drainage capabilities.

This study explores the permeability and stiffness properties of porous asphalt mixtures in a laboratory setting, analyzing these properties as a function of mixture porosity. For two types of pavement mixtures, four target porosity levels were evaluated: 19%, 18%, 17%, and 16%. These levels represent the range of porosity that porous pavement materials are expected to exhibit during their service life, corresponding to their permeability coefficients (hydraulic conductivity). The constant-head test was used to determine the permeability coefficient, while the resilient modulus was measured to assess stiffness performance. The study compares the permeability and stiffness characteristics of the two types of porous pavement materials.

2. Materials used in the study

2.1. Aggregate

The properties of aggregates significantly impact the performance of the binder. Aggregates must meet stringent specifications and be free from chemicals, clay coatings, and other fine materials that could impede the asphalt binder's hydration and bonding process. Additionally, the aggregates must be clean, durable, and robust.

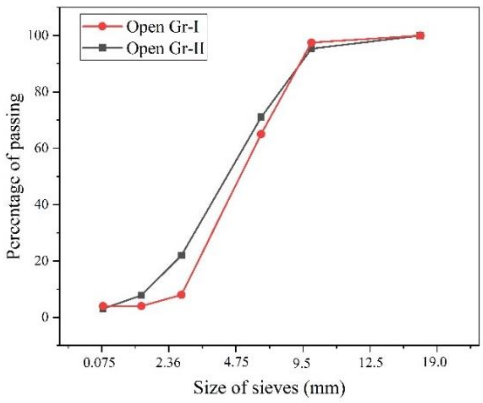

Fig. 2. Gradation curve used for this study.

The gradation bandwidth was chosen according to the National Asphalt Pavement Association (NAPA) specifications. The natural coarse aggregates used in this study comprised siliceous and calcareous materials, with a maximum size of 19 mm and a specific gravity of 2.66. Two different binders were employed, and two distinct porous asphalt mixtures with nominal maximum aggregate sizes (NMAS) of 19 mm and open-graded gradations were used. These gradations were based on aggregate packing studies. [38]. The two gradations impacted the initial air voids, affecting the asphalt mixtures' permeability. The bitumen composition for each intended gradation, the placement of the coarse and fine aggregates, and the specified percentage for mixing are outlined below. The mixtures were compacted at temperatures of 150-153°C and 162-164°C. Figure 2 displays the open gradation considered in this study. Open gr-I is a coarse gradation comprising 80-85% of the maximum aggregate size, while Open gr-II is a fine gradation containing 22% of fine sizes, as determined by packing studies.

2.2. Specifications of mixture binder

The previous study describes the methodology used for designing the mixture in this research. A porous asphalt mixture was successfully created using PMB40 asphalt binder, modified with styrene-butadiene-styrene (SBS) and VG30 (viscosity grade bitumen), as detailed in Tables 1 and 2. According to the NAPA standards, porous asphalt concrete's nominal maximum aggregate size is less than 19 mm. Specimens ranging from 101.5 mm to 63.5 mm were produced using the Marshall Mix design. This study compared a medium-viscosity binder with a polymer-modified high-viscosity binder to analyze its effects on drainage properties and stiffness parameters.

Table 1. PMB40 Binder properties.

S.No	Characteristics of PMB40	Results	IS 15462:2004
1	A penetration test, 25ºC.0.1mm,100g	42	30 to 50
2	Softening point test	64	Min. 60°C
3	Elastic Recovery test	80	Min. 70%
4	Viscosity test	5.6	3-9 poise
5	Separation test	1	Max 3°C
6	Tests on residue from RTFOT		
	a) Loss in mass	0.8	1.0% Max
	b) Softening point test	3	5 °C Max
	c) Reduction in Penetration	27	35% Max

Table 2. VG30 Binder properties.

S.No	Test	Results	IS73 (2018)
1	Absolute viscosity at 60ºC (poise)	2765	2400-3600
2	Kinematic viscosity at 135ºC (centistokes)	399.0	350 Min.
3	Penetration point 25ºC.0.1mm,100g	50.0	45 Min.
4	Softening point ºC	53.0	47 Min

3. Research problem

The main goal of the research was to investigate how aggregate gradation impacts the permeability and stiffness characteristics of porous asphalt mixtures. The study involved preparing mixtures using two different gradations and binders, evaluating their drainage properties, and assessing the material's stiffness under various conditions. Pore structure analysis was conducted using image analysis techniques, and a 3D model was developed for this purpose. Permeability data compare with different air void content in the mix.

4. Research methodology

The MR test is a standardized method used to assess the mechanical properties of asphalt samples. This dynamic shear test evaluates the asphalt's capacity to withstand deformation and regain its original shape after experiencing stress. The primary goal of the current research is to compare the permeability and stiffness characteristics of two porous pavement materials: VG30 and PMB40. The permeability coefficient is utilized as the drainage parameter to describe the ability of the porous materials to drain. These materials are assessed to determine their MR and permeability coefficient at various stages. Additionally, air void content is measured to analyze the stiffness behavior of each tested porous specimen.

5. Test performance

5.1. Permeability test set-up

Permeability is a critical characteristic between conventional and porous asphalt mixtures; this is also the main distinction. The analysis of these mixes must include a method for accurately measuring this feature. It was necessary to devise new techniques for calculating drainage capacity. Per Darcy's law, a prototype model is developed in the laboratory to measure the falling head permeability, as shown in Figure. 3.

$$K = 2.3\frac{aL}{\mathrm{Al}}\log\left(\frac{h1}{h2}\right) \quad (1)$$

where k is the coefficient of permeability (cm/s), A is the cross-section area of the specimen (cm2), a is the cross-section area of the standpipe (cm2), L is height of specimen (cm), t is time taken for water in the standpipe to fall from h1 to h2(s), h1 is head at the beginning of time measurement (cm), h2 is the head at the end of time measurement (cm). Equation (1) was developed based on Darcy’s law, which assumed that the sample was saturated and homogenous while the flow was laminar. There have been some arguments about the applicability of Darcy’s law for calculating the coefficient of permeability in the context of porous asphalt. Darcy’s law remains valid. (Tan et al. And Fwa et al. 2013).

To investigate the seepage characteristics of porous asphalt mixes, the permeability of each sample in the Open gradation Gr-I and Gr-II series was analyzed. Initial permeability values for new porous asphalt surfaces ranged from 0.4 to 0.294 cm/sec. Permeable pavement, characterized by a porous surface made of an asphalt sample, was the focus of this study. A laboratory-constructed falling head permeability test device was developed, featuring a 100mm diameter standpipe, two glass plates positioned in a 100mm diameter asphalt mold, and a control chamber ball valve connected to the standpipe. Additionally, the study examined the sudden on/off flow to the sample, facilitated through a ball valve mechanism.

Fig. 3. In-House Fabricated Permeability Test Set-up.

5.2. Resilient modulus test

The ASTM D7369 – 20 procedure outlines testing resilient modulus (MR) by specifying the load, frequency, and duration. This procedure was followed for testing at five distinct temperatures: 5°C, 15°C, 20°C, and 25°C. The Indirect Tensile Strength (ITS) is also measured at 25°C using a temperature-controlled chamber. For MR testing, the ITS results indicate a binder content range of 10% to 20%. Laboratory cores should be heated to the test temperature in a controlled chamber. To ensure accuracy, core specimens must be maintained at 25°C for at least 6 hours before testing unless another precise temperature monitoring method is used. It's also recommended that a dummy sample be used to verify temperature and ensure proper specimen seating and alignment. The test specimen should be positioned such that the mid-thickness mark, where the two diametric axes intersect, aligns with the actuator shaft or is perfectly centered between the end markings of the loading strips. Proper alignment is crucial, and the back face of the specimen can be inspected using a mirror. The contact surface of each loading strip with the specimen must be flawless for accurate results. For preconditioning, apply 100 load applications per rotation. However, the minimum load applications needed should be chosen based on maintaining consistent deformations in the resilient modulus. At least five stable processes are required where the resilient modulus change is less than 1% over five consecutive cycles. Record the cause and number of preconditioning cycles if additional methods are used. If total cumulative vertical deformations exceed 0.025 mm (0.001 in.), reduce the applied load to the minimum level necessary to maintain measurable deformations. After preconditioning, record deformation measurements separately from the load sensor and four deformation measuring devices. The last five loading cycles are used for recording responses, including deformation and load. Each loading cycle consists of a load pulse followed by a rest period. This process assesses the strength of the specimen under tension. Ensure the loading axis of the specimen is aligned with its initial testing position. Calculate the total MR (MPa), sample thickness (mm), and Poisson's ratio (μ) using the appropriate equation.

$$MR = \frac{P}{Ht}(0.27 + \mu) \quad (2)$$

6. Results and analysis

6.1. Pore structure analysis

The plane and three-dimensional porosity measurement methods were employed and compared for the porosity analysis. A summary of the research findings is provided in Table 3, which will be discussed in the next section. The results indicate that porosity in specimens can be measured accurately using ImageJ techniques. When using this image measurement method, it is important to consider that the results are significantly affected by the clarity of the scanned CT slice and the chosen threshold Figures 4 and 5 show different pore structures and associated voids. There is a link between aggregate gradation and pore structure. Red markings highlight the pore structure in the compacted sample. Particle analysis of total permeability simulation was performed to examine how material permeates the internal voids of the PAM. This simulation accounted for the materials' multi-scale and multi-directional flow characteristics within the PAM's pores.

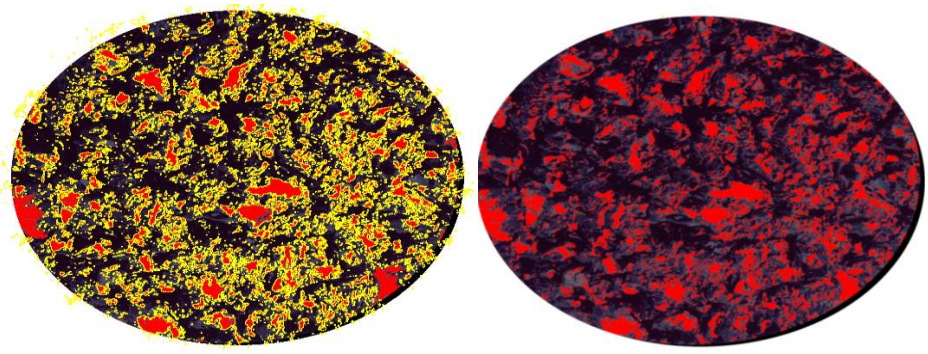

Fig. 4. Connected pore structure of the Porous sample **(Top view).**

Two binders differ in air void content in mx—open Gr-I high air void content combination of VG30.Pore size is also high in the mixture, influenced by coarse aggregate percentage. The connected pore structure of the specimen combined layer structure was developed during the first image analysis phase. It indicates the air voids skeleton. The second phase is the labeling of pores and separation of each layer, as well as a clear indication of aggregate structure with coated bitumen. The third image analysis phase developed a pore structure model and neglected the coated aggregate structure.

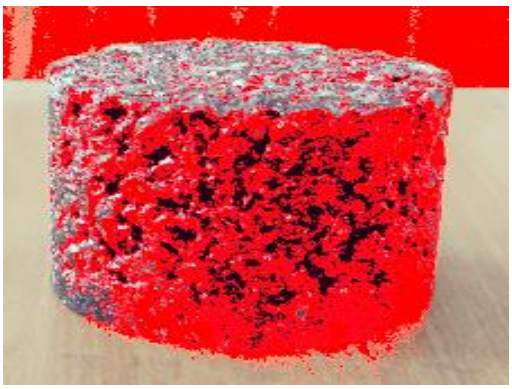

Fig. 5. Internal view of connected air voids.

Table. 3. Results of pore dimensions.

Description	VG 30		PMB 40	
	Open Gr-I	Open Gr-II	Open Gr-I	Open Gr-II
Pore structure total	2.489	2.496	2.474	2.483
Pore structure (Connected)	2.428	2.424	2.389	2.418

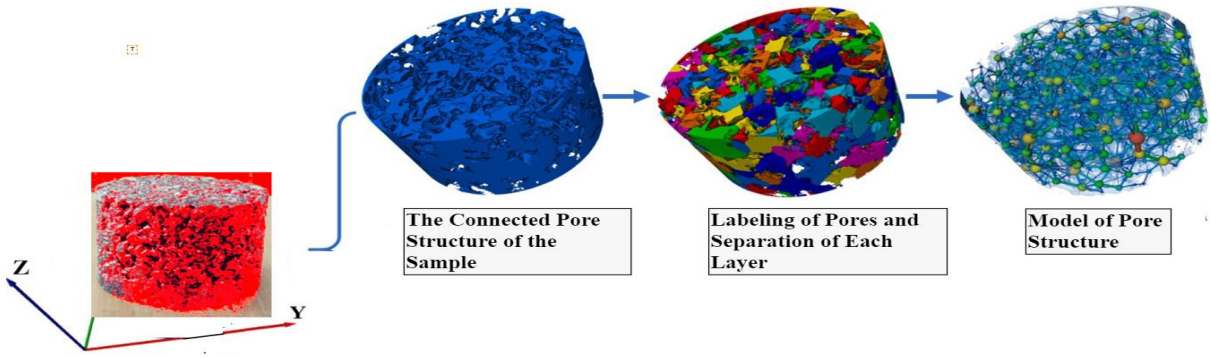

Fig. 6. Analysis of the pore structure in three dimensions.

The notable increase in the infiltration rate of porous materials attributed to PAM is not primarily due to overall porosity but rather the connected porosity. This study employs the connected porosity ratio, which is the ratio of connected porosity to total porosity. Figure 6 illustrates the connectivity of PAM voids. Although there are some discrepancies between measurements obtained using the 3D measurement method and the water displacement method, both methods reveal a similar trend: the connected porosity ratio of PAM increases as the PAM content rises. As the aggregate size of PAM increases, the connected pore ratio also increases, even if the overall porosity remains constant. This observation supports the idea that increasing PAM's porosity and aggregate size enhances pore connectivity. Table 03 presents the results related to pore dimensions.

6.2. Coefficient of permeability

The permeability of the porous asphalt samples was assessed using a falling head permeameter. Permeability refers to the rate at which water can pass through a porous material. For effective pavement performance, it is essential that water can flow through and away from the surface at an appropriate rate. According to [37], a minimum permeability rate of 100 m/day (0.115 cm/sec) is required for proper pavement functionality. Despite its importance, porous asphalt (PA) mix design typically relies on indirect indicators such as minimum total air void content or optional permeability assessments of lab-produced samples. However, other factors also influence the performance of PA mixtures in terms of permeability, including the quantity, area, and equivalent diameter of voids, which are significant volumetric characteristics.

Fig. 7. a) porous asphalt sample ready for test; b) 24-hour saturation before conducting a test (permeameter filled with water).

Figure 7 depicts the sealed sample ready to be tested using the in-house produced permeameter before the test was conducted. The sample was kept in the temperature chamber of the UTM for four hours at 25 degrees. Following conditioning, the specimen will be fixed in the permeameter stand before the test. Once saturation is completed, the sample is ready for the cycle permeability test. The sample kept two

Perspex plates attached screws are used to tighten the sample specimen along with rubber rings. Rubber rings are essential to house fabricated equipment because of water leakage on the mould sides.

The results of the current study showed that Gr-II had less porosity than open Gr-I; this indicated that Gr-II's lower permeability was anticipated. The fine gradation resulted in aggregate particles that were packed more tightly in comparison to the coarser gradations, which resulted in a lower air void content in Gr-II and, as a consequence, a lower permeability in the Open Gr-II category, which is the category with the highest porosity, experienced the most significant improvement in permeability as shown in Figures 8 and 9, respectively. Here, the permeability coefficient occurred between 280 and 360 meters/day, indicating that the porous structure performs well regarding drainage quantification. Air void content effect Open gr-I in combination with medium viscosity binder influences the permeability value. The drainage parameter in a porous asphalt mixture is high in the mix. Polymer-modified binder mixture in open Gr-II has a low permeability value in the effect of aggregate gradation, and binder film thickness affects the air void content in the mix.

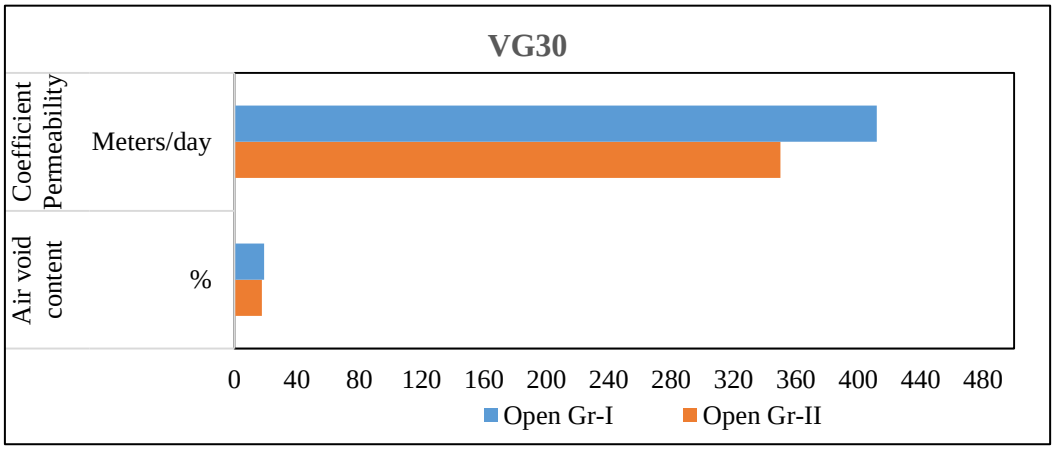

Fig. 8. Coefficient of Permeability vs Air void content of VG30 binder Open Gr- I & I.

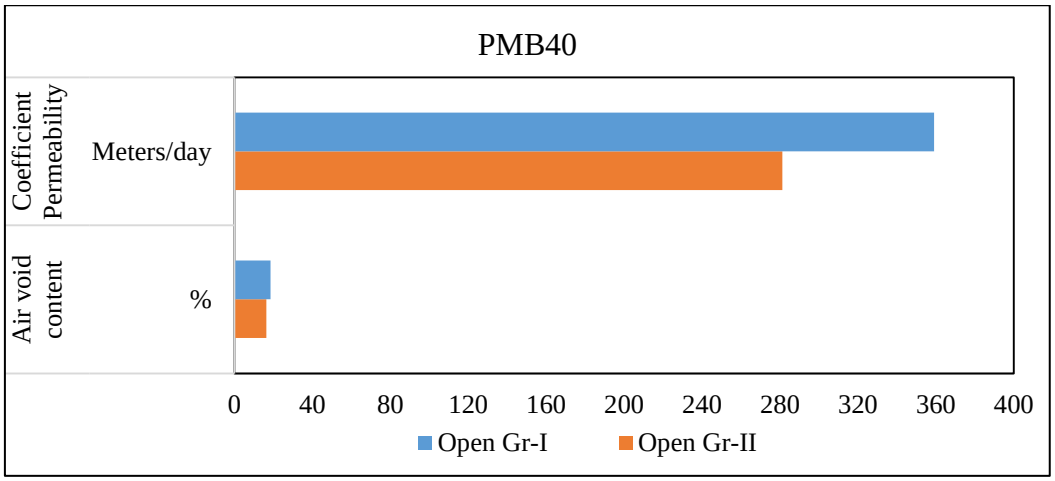

Fig. 9. Coefficient of Permeability vs Air void content of PMB40 binder Open Gr- I & II.

Porosity can be considered a structure of voids permeable to water from the outside; nevertheless, permeability is more closely associated with porosity than air voids. Calculating the permeability of an aggregate mixture is attainable if one considers the void ratio of the aggregate gradation. This is done According to the connections between permeability and the time it takes water to pass through a porous asphalt specimen, as depicted in Figure 10. Permeability values are correlated with the time in seconds, and water head height also influences the time of drain out. An aggregate skeleton or structure primarily depends on two forms of the porous skeleton: their size, shape, and texture. Here, the vital role of Gr-I

combinations is to have higher permeability rates due to more air voids. The Interconnecting voids that allow water to pass through an open Gr-II mixture are reduced when the fine content is high since this tends to fill more void spaces. High acceptable content also leads to an increase in mastic. Also, two gradations reached the maximum permeability value.

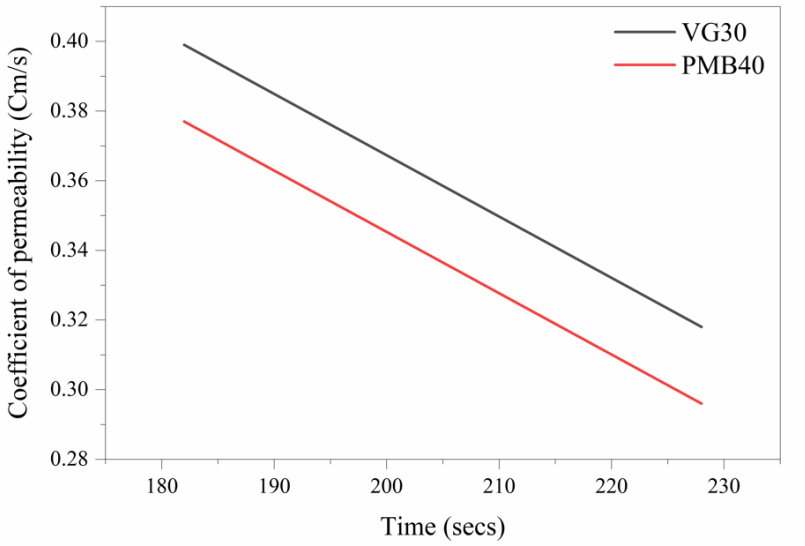

Fig. 10. Coefficient of permeability with time Open Gr- I & II.

6.3. Indirect tensile strength (ITS)

This test was carried out per ASTM D 6931-07 and involved loading a Marshall specimen with a single load in a direction perpendicular to the vertical diametral plane. During the test, strain gauges were utilized to measure the horizontal deformation at the highest load. To evaluate how the mix behaves at lower temperatures, the test is carried out at 25 degrees Celsius. The following equation (1) describes tensile strength as well as the tensile strain at the point of failure:

$$T_s = \frac{2000P}{\pi dt} \quad (1)$$

Where Ts is ITS (Kpa), P is applied load (N),d is the diameter of the specimen, and t is the thickness of the specimen. After conducting ITS, it took 10 to 20% of the value of ITS to conduct a resilient modulus ($M_{R)}$ test. The ITS values used for the study's resilient modulus are shown in Figure 11. This study considers 15% of the ITS value for the M_R test.

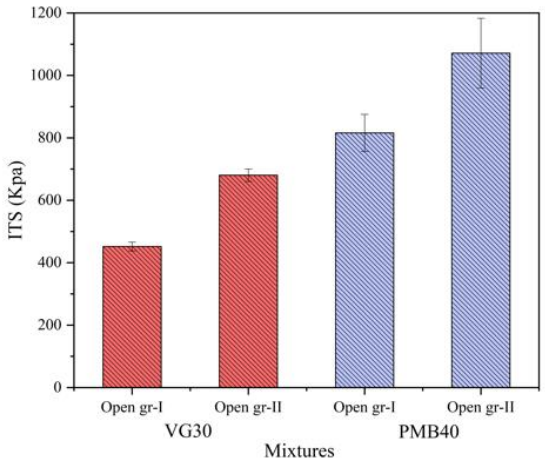

Fig. 11. Trend of indirect tensile strength values for the mixes.

6.4. Resilient modulus

The resilient modulus, evaluated in the indirect tensile mode, accurately represents the elastic properties that asphalt mixtures exhibit when subjected to repeated stress. In the past, one of the most common approaches to determining the stiffness modulus of hot-mix asphalt was to use the resilient modulus. The M_R values occurred at 2200 and 2500 for VG30 binders, which showed that these types of surface courses have more stiffness for external and impact loads. Figure 12 shows the specimen set in a UTM machine with LVDTs and ready for testing in the temperature chamber.

Fig. 12. Resilient modulus test sample set up in the equipment.

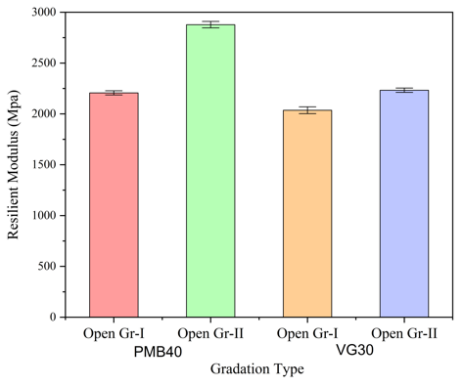

Fig. 13. Resilient modulus values for Open Gr- I & II.

Here is the resilient data for each gradation. The maximum value of the M_R list is below. The porous structure cyclic load force gradually increased in the five cycles illustrated below. Figure 13 shows the differences in resilient modulus with permissible content, binder quality, and compaction level porous.
The indirect tensile strength test carried out as part of the research project revealed that the results for resilient modulus also suggested that mixtures with virgin binder show greater resilient modulus values. Virgin binder values are lower than a modified binder (PMB40). Both of these findings can be found in the study. This leads to more rigid mixtures with a larger capacity to spread loads and more excellent resistance to fatigue cracking and irreversible deformation structure modular value, which is higher for these two open gradations.

Fig. 14. UTM test equipment set up, including temperature chamber.

High and medium viscous binders have proven essential in strengthening the resistance of asphalt mixes to various stresses, even though these binders only make up a small part of the overall mixture. The presence of changed binders can benefit the combination's overall performance, particularly its strength, stability, and resilient modulus. The UTM testing equipment is seen in Figure 14. The last five cycles of data are presented in Tables 04 and 05 of different mixtures.

Table 4. Resilient modulus test data for the last five cycles for PMB40.

Cycle		1	2	3	4	5	Mean	SD	CV%
MR	MPa	3584.98	3467.55	3502.50	3460.88	3452.13	3493.61	48.78	1.40
CLF	N	1286.16	1333.62	1351.47	1347.35	1352.85	1334.29	25.01	1.87
CF	N	20.14	19.99	19.99	19.99	19.99	20.02	0.06	0.30
TRHD	µm	3.53	3.78	3.80	3.83	3.86	3.76	0.12	3.12

MR Resilient Modulus; CLF Cyclic Loading Force; CF Contact force and TRHD Total recoverable horizontal deformation

Table 5. Resilient modulus test data for the last five cycles for VG30.

Cycle		1	2	3	4	5	Mean	SD	CV%
MR	MPa	2405.77	2305.12	2267.39	2279.52	2239.33	2299.43	57.23	2.49
CLF	N	1178.74	1251.53	1267.24	1269.84	1268.92	1247.25	34.90	2.80
CF	N	20.14	20.45	19.84	19.53	20.14	20.02	0.31	1.55
TRHD	µm	4.28	4.74	4.88	4.86	4.95	4.74	0.24	5.09

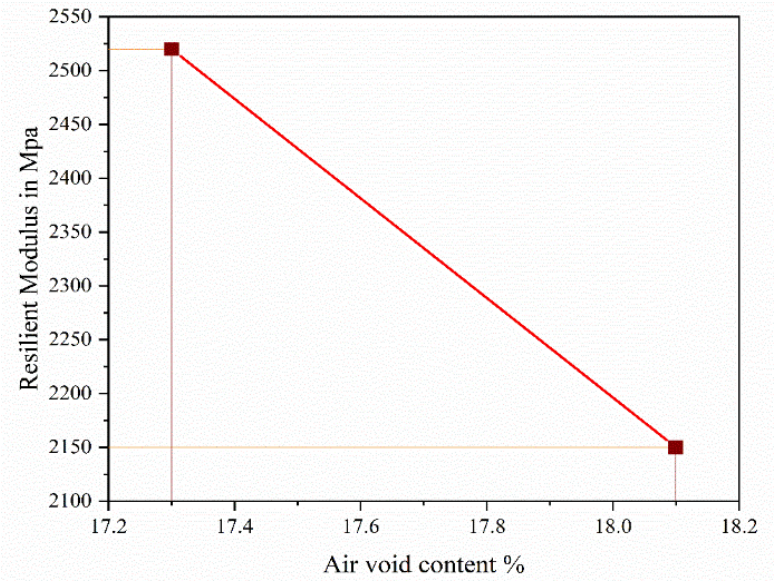

Fig. 15. Influence of air void content in MR (VG30).

This test will measure the stiffness of porous asphalt mixtures. Repeated haversine waveform compressive loads were applied to the sample at 25 °C. Figures 15 and 16 depict the results of a resilient modulus test at 25°C utilizing two unique gradations and two different binders. The results show that the mixture with Porous Gradation Open Gr-II has the highest resilient modulus when tested at 25 °C compared to mixes with PMB40 greater than VG30. As a result, when compared to a mixture that contains fewer than 10% particles, the combination increases the stiffness of porous asphalt mixes. As a result, a relationship between the high strength modulus and the air void concentration has been determined. Overall, it is evident that the starting value increases while the resilient modulus decreases with increasing void content.

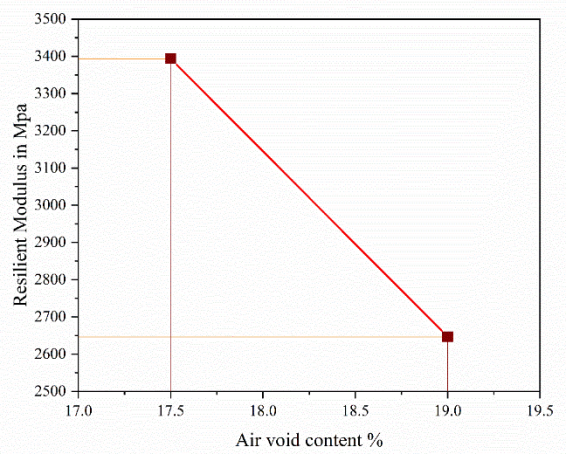

Fig. 16. Influence of air void content in MR (PMB40).

6.4.1. Effect of different optimum binder content on resilient modulus

The influence that varying amounts of binder have on the resilient modulus is depicted in Figure 17. According to the compiled results, it appeared as though the resilient modulus was high when the binder concentration was 5.5 percent. Still, it became lower when the binder level was 5.9 percent. An increase in the amount of binder used could have s. Researchers discovered that materials with a high binder concentration achieved the lowest resilient modulus possible. On the other hand, it was found that the modulus of the mix with particular binder contents had a value that decreased over time. This suggested that the tests did not follow a linear procedure as far as the damage accumulation of the material was concerned.

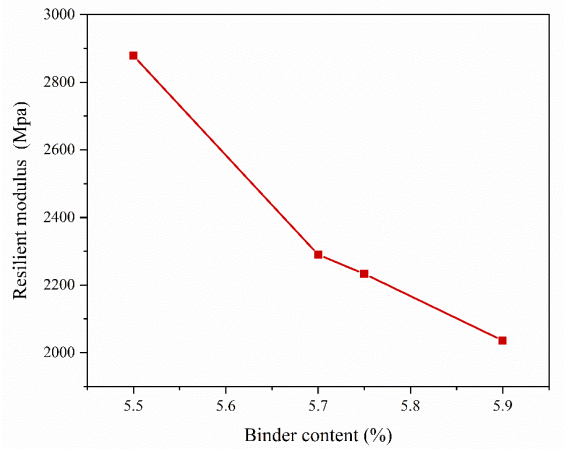

Fig. 17. Trend of resilient modulus at different binder content.

7. Horizontal deformation vs load for mixtures

The stiffness modulus of the asphalt mixtures was analyzed with the help of a durable modulus test, which was carried out with the help of the repeated-load indirect tension test. The testing procedure is a non-destructive approach to establish whether a combination may recover after being subjected to repeated stress. Results with a high resilient modulus value demonstrate that the asphalt mixture is stiff and that less strain may be retrieved from repeated vehicle loads. This indicates that the variety is more resistant to cracking. Peak loads were applied periodically to the cylindrical samples throughout this test, resulting in horizontal deformations of 200 and 300 macro stresses. In each load cycle, a 0.9-s rest period comes after a 0.1-s load application. It is possible to determine the resilient modulus over some time by continually measuring the load and the deformation. Additionally, the specimen axis and the degree of

grain-to-grain contact between aggregates in a porous structure are factors that impact the deformation of the material. The characteristics of stiffness were the primary focus of the current investigation because of the durability assessment they provide. The information presented in Figures 18 and 19 demonstrates that the PMB 40 and VG30 binder combination of open Gr-II is more durable than Gr-I, which is currently available. The gradation sizes, the structure aggregate skeleton, and the axis of direction sample are the factors that significantly influence the outcome. In Open Gr-I, the horizontal deformation value has a more significant impact on the VG30 medium viscosity binder, and the air void content of the mix is higher than in other combinations. The layer thickness of the binder film affects the deformation of the compacted structure. Open Gr-II combination of polymer-modified binder deformation on the lower side compared to other porous asphalt mixtures in the selected gradations. The last five cyclic loading periods measure the horizontal deformation of the compacted specimen in the laboratory. The PMB40 combination of a mix of Open Gr-II has a higher stiffness value.

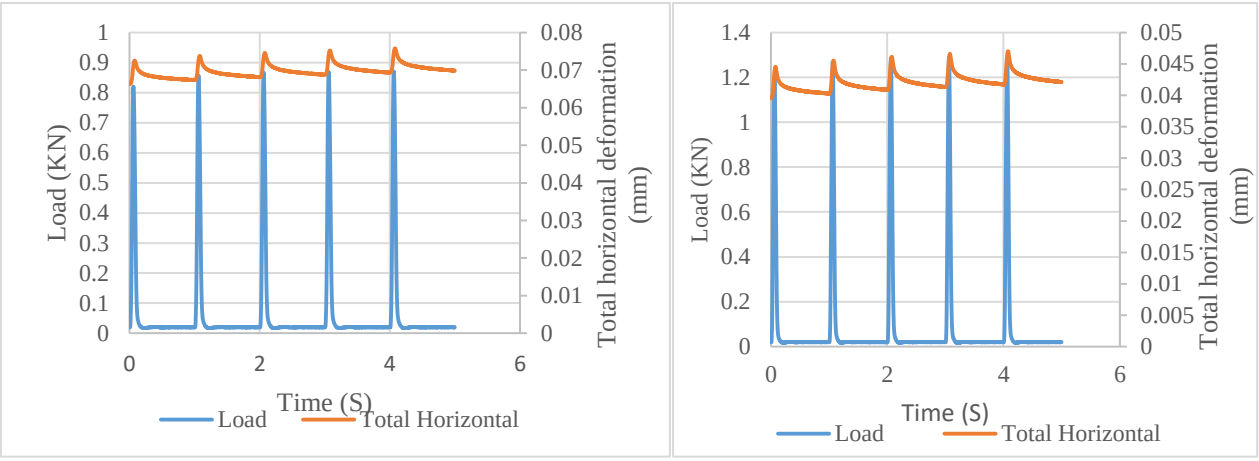

Fig. 18. Load vs Total horizontal deformation of VG30 binder Open Gr- I & II.

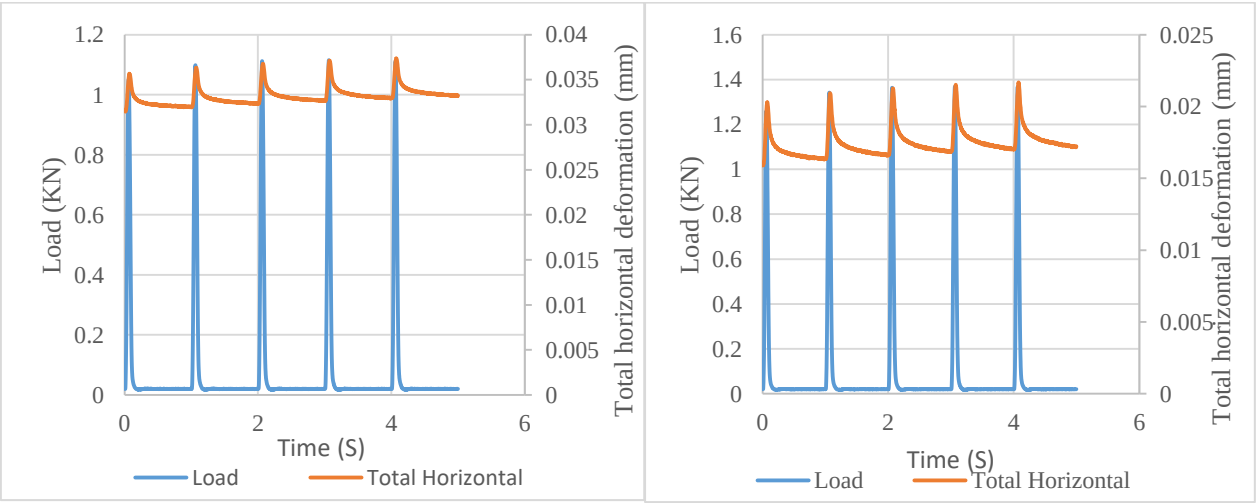

Fig. 19. Load vs Total horizontal deformation of PMB40 binder Open Gr- I & II.

8. Conclusions

Based on the results obtained from the analysis and developed models in the present study, the following conclusions are drawn:

- Gradation, skeleton mass, and binder film thickness all play a role in determining permeability. Both binders exhibit high permeability values, with open Gr-I at 0.4 cm/sec and open Gr-II at

0.290 cm/sec. PAM porosity and aggregate size significantly impact pore structure complexity. Generally, simpler porous structures exhibit higher porosity and larger aggregate sizes. PA mixes present a variety of total, connected, and distributed pore structures.

- Air void content substantially affects the permeability of modified binders, influencing each mixture by approximately 20%. Factors such as the gradation of open-graded mixtures, the type and content of binder, and mixing and compaction temperatures play a crucial role in this influence.
- An increase in air void content across two gradations, leads to a decrease in resilient modulus, as fines and filler materials constitute less than 10%. Open Gr-I shows a lower modulus value of 2150 MPa for the VG30 binder, while open Gr-II records a higher modulus value of 3350 MPa for the PMB40 binder.
- The stiffness requirements are met for both open Gr-I and Gr-II mixtures, with VG30 and PMB40 binders used during critical load cycles. The porous asphalt gradation demonstrates strong average modulus values above 1500 Mpa. Polymer-modified asphalt enhances the cohesion and durability of porous asphalt mixtures, facilitating the achievement of the desired binder film thickness.
- VG30 binders exhibit a high resilience modulus due to their optimal pore sizes and aggregate dimensions. The percentage of each grade impacts the mixes significantly. There is an interaction between permeability and stiffness, with high permeability influencing the modulus value.

9. Recommendations of study

In porous asphalt pavement, the most crucial phase is to carry out the test in a variety of coupled conditions, including the following instances: In the future, the scope of the study will expand to include permeability tests carried out at varying temperatures as well as variations in the effects of compaction in test samples of porous asphalt mixture. The compaction effect is compared with the mix's permeability and air void content. Calculate the refusal density percentage of each mixture.

Conflicts of Interest

The authors declare no known competing financial interests or personal relationships that could have influenced the work reported in this paper.

The author is an Editorial Board Member/Editor-in-Chief/Associate Editor/Guest Editor for [Journal of Rehabilitation in Civil Engineering] and was not involved in the editorial review or decision to publish this article.

Funding

This research received no specific grant from funding agencies in the public, commercial, or not-for-profit sectors.

Author’s contribution statement

Chiranjeevi Gummadi: Conceptualization, writing-original draft, Investigation, Methodology, Writing-review, Investigation.

S Shankar: Methodology, review, Conceptualization.

Reference

[1] Hosokawa H, Gomi A, Tamai A, Kasahara A. Hot in-place recycling of porous asphalt concrete. 4th Int Conf Maint Rehabil Pavements Technol Control MAIREPAV 2005 2005:1–9.

[2] Hardiman M. Y. The Comparison of Engineering Properties Between Single and Double Layer Porous Asphalt made of Packing Gradation. Civ Eng Dimens 2008;10:82–8.

[3] Norazman C, Wan C, Jaya RP, Hamzah MO. Properties of Porous Asphalt Mixture Made With Styrene Butadiene Styrene under Long Term Oven Ageing 2012;486:378–83. https://doi.org/10.4028/www.scientific.net/AMR.486.378.

[4] Kamboozia N, Rad SM, Saed SA. Laboratory Investigation of the Effect of Nano-ZnO on the Fracture and Rutting Resistance of Porous Asphalt Mixture under the Aging Condition and Freeze – Thaw Cycle 2022;34:1–17. https://doi.org/10.1061/(ASCE)MT.1943-5533.0004187.

[5] Pouranian MR, Imaninasab R, Shishehbor M. The effect of temperature and stress level on the rutting performance of modified stone matrix asphalt 2020. https://doi.org/10.1080/14680629.2018.1546221.

[6] Nadeem M, Al-shamrani AM, Jameel M, Khan NA, Ibrahim Z, Akhtar JN. Case Studies in Construction Materials Stability and permeability characteristics of porous asphalt pavement : An experimental case study. Case Stud Constr Mater 2021;15:e00591. https://doi.org/10.1016/j.cscm.2021.e00591.

[7] Nahar S, Mohajeri M, Schmets A, Scarpas A, Van De Ven M, Schitter G. First observation of blending-zone morphology at interface of reclaimed Asphalt Binder and Virgin Bitumen. Transp Res Rec 2013:1–9. https://doi.org/10.3141/2370-01.

[8] Briggs JF. Performance Assessment of Porous Asphalt for Stormwater Treatment 1996.

[9] Ma X, Li Q, Cui YC, Ni AQ. Performance of porous asphalt mixture with various additives. Int J Pavement Eng 2018;19:355–61. https://doi.org/10.1080/10298436.2016.1175560.

[10] Mohd Shukry NA, Hassan NA, Abdullah ME, Hainin MR, Md Yusoff NI, Jaya RP, et al. Effect of various filler types on the properties of porous asphalt mixture. IOP Conf Ser Mater Sci Eng 2018;342. https://doi.org/10.1088/1757-899X/342/1/012036.

[11] Nakanishi H, Hamzah MO, Mohd Hasan MR, Karthigeyan P, Shaur O. Mix design and application of porous asphalt pavement using Japanese technology. IOP Conf Ser Mater Sci Eng 2019;512. https://doi.org/10.1088/1757-899X/512/1/012026.

[12] Yang B, Li H, Zhang H, Xie N, Zhou H. Laboratorial investigation on effects of microscopic void characteristics on properties of porous asphalt mixture. Constr Build Mater 2019;213:434–46. https://doi.org/10.1016/j.conbuildmat.2019.04.039.

[13] Sangiorgi C, Eskandarsefat S, Tataranni P, Simone A, Vignali V, Lantieri C, et al. A complete laboratory assessment of crumb rubber porous asphalt. Constr Build Mater 2017;132:500–7. https://doi.org/10.1016/j.conbuildmat.2016.12.016.

[14] Hagos ET, Molenaar AAA, Van De Ven MFC, Voskuilen JLM. Durability related investigation into porous asphalt. Adv Characterisation Pavement Soil Eng Mater - Proc Int Conf Adv Characterisation Pavement Soil Eng Mater 2007;1:713–27.

[15] Afonso ML, Dinis-Almeida M, Fael CS. Study of the porous asphalt performance with cellulosic fibres. Constr Build Mater 2017;135:104–11. https://doi.org/10.1016/j.conbuildmat.2016.12.222.

[16] Slebi-Acevedo CJ, Castro-Fresno D, Pascual-Muñoz P, Lastra-González P. A combination of DOE–multi-criteria decision making analysis applied to additive assessment in porous asphalt mixture. Int J Pavement Eng 2021;0:1–14. https://doi.org/10.1080/10298436.2020.1859508.

[17] Alvarez AE, Martin AE, Estakhri C. A review of mix design and evaluation research for permeable friction course mixtures. Constr Build Mater 2011;25:1159–66. https://doi.org/10.1016/j.conbuildmat.2010.09.038.

[18] Chu L, Fwa TF. Functional sustainability of single- and double-layer porous asphalt pavements. Constr Build Mater 2019;197:436–43. https://doi.org/10.1016/j.conbuildmat.2018.11.162.

[19] Ma Y, Chen X, Geng Y, Zhang X. Effect of Clogging on the Permeability of Porous Asphalt Pavement. Adv Mater Sci Eng 2020;2020. https://doi.org/10.1155/2020/4851291.

[20] Kathryn L. Porous Asphalt Pavement designs: Proactive design for cold climate use 2007:105.

[21] Alves T da CL, Shah N. Construction Research Congress 2018. Proceeding Constr Res Congr 2018 2018;1996:148–57.

[22] Conzelmann NA, Partl MN, Clemens FJ, Müller CR, Poulikakos LD. Effect of artificial aggregate shapes on the porosity, tortuosity and permeability of their packings. Powder Technol 2022;397. https://doi.org/10.1016/j.powtec.2021.11.063.

[23] Peng B, Han S, Han X, Zhang H. Laboratory and field evaluation of noise characteristics of porous asphalt pavement. Int J Pavement Eng 2021;0:1–14. https://doi.org/10.1080/10298436.2021.1893319.

[24] Chu L, Tang B, Fwa TF. Evaluation of functional characteristics of laboratory mix design of porous pavement materials. Constr Build Mater 2018;191:281–9. https://doi.org/10.1016/j.conbuildmat.2018.10.003.

[25] Fwa TF, Lim E, Tan KH. Comparison of permeability and clogging characteristics of porous asphalt and pervious concrete pavement materials. Transp Res Rec 2015;2511:72–80. https://doi.org/10.3141/2511-09.

[26] Garcia A, Aboufoul M, Asamoah F, Jing D. Study the influence of the air void topology on porous asphalt clogging. Constr Build Mater 2019;227:116791. https://doi.org/10.1016/j.conbuildmat.2019.116791.

[27] Frigio F, Pasquini E, Ferrotti G, Canestrari F. Improved durability of recycled porous asphalt. Constr Build Mater 2013;48:755–63. https://doi.org/10.1016/j.conbuildmat.2013.07.044.

[28] Khosla N, Birdsall BG, Kawaguchi S. Evaluation of Moisture Susceptibility of Asphalt Mixtures: Conventional and New Methods. Transp Res Rec J Transp Res Board 2000;1728:43–51. https://doi.org/10.3141/1728-07.

[29] Watson DE, Cooley LA, Moore KA, Williams K. Laboratory performance testing of open-graded friction course mixtures. Transp Res Rec 2004:40–7. https://doi.org/10.3141/1891-06.

[30] Gupta A, Castro-Fresno D, Lastra-Gonzalez P, Rodriguez-Hernandez J. Selection of fibers to improve porous asphalt mixtures using multi-criteria analysis. Constr Build Mater 2021;266:121198. https://doi.org/10.1016/j.conbuildmat.2020.121198.

[31] Cetin A. Effects of crumb rubber size and concentration on performance of porous asphalt mixtures. Int J Polym Sci 2013;2013. https://doi.org/10.1155/2013/789612.

[32] Shirini B, Imaninasab R. Performance evaluation of rubberized and SBS modified porous asphalt mixtures. Constr Build Mater 2016;107:165–71. https://doi.org/10.1016/j.conbuildmat.2016.01.006.

[33] Wang S, Kang A, Xiao P, Li B, Fu W. Investigating the effects of chopped basalt fiber on the performance of porous asphalt mixture. Adv Mater Sci Eng 2019;2019. https://doi.org/10.1155/2019/2323761.

[34] Alber S, Ressel W, Liu P, Wang D, Oeser M. Influence of soiling phenomena on air-void microstructure and acoustic performance of porous asphalt pavement. Constr Build Mater 2018;158:938–48. https://doi.org/10.1016/j.conbuildmat.2017.10.069.

[35] Zhao Y, Huang X. Design method and performance for large stone porous asphalt mixtures. J Wuhan Univ Technol Mater Sci Ed 2010;25:871–6. https://doi.org/10.1007/s11595-010-0111-2.

[36] Dietz ME. Low impact development practices: A review of current research and recommendations for future directions. Water Air Soil Pollut 2007;186:351–63. https://doi.org/10.1007/s11270-007-9484-z.

[37] Watson DE, Moore KA, Williams K, Cooley LA. Refinement of New-Generation Open-Graded Friction Course Mix Design. Transp Res Rec 2003:78–85. https://doi.org/10.3141/1832-10.

[38] Chiranjeevi G, Shankar S. Evaluation of different porous asphalt gradations based on aggregate packing and stiffness parameters. Innov Infrastruct Solut 2022. https://doi.org/10.1007/s41062-022-00969-8.